

Atmospheric Transparency Changes Associated with Solar Wind-Induced Atmospheric Electricity Variations.

V. C. Roldugin[#] and B. A. Tinsley*

[#]*Polar Geophysical Institute, Apatity, Russia*

**University of Texas at Dallas, FO22, Richardson, TX, 75083-0688, USA*

**Corresponding author, Tinsley@UTDallas.edu, Tel. 972 883 2838, Fax 972 883 2761*

Abstract

Variations in atmospheric transmission of several percent in nominally clear air are found to accompany solar wind events associated with variations on the day-to-day timescale in the flow of vertical current density (J_z) in the global electric circuit. The effect has been observed only for stations at high latitudes ($>55^\circ\text{N}$). Increases in transmission are present when inferred J_z decreases occurred without changes in tropospheric ion production. These events occurred when there was a high loading of stratospheric aerosols. Responses of opposite sign, i.e., decreases in transmission, are present when Forbush decreases of galactic cosmic ray flux occur, but only during periods of low stratospheric aerosol loading. Forbush decreases are associated with both tropospheric ion production decreases and J_z decreases. Similar effects are present on the 11-year solar cycle, with climate consequences that have yet to be analyzed. The mechanisms for these phenomena are not understood, but the nature of the observations suggests that explanations should be sought in terms of theories of the effects of electric charge on the formation of aerosols, and/or effects of charged aerosols on the microphysics of vapor-water-ice conversions.

Keywords: Atmospheric ionization, Atmospheric transparency, Aerosols, Climate

1. Introduction

The dominant source of ionization and conductivity in the troposphere and stratosphere is the flux of galactic cosmic rays (GCR) that is modulated by varying magnetic fields in the supersonic solar wind, and filtered in energy by the geomagnetic field (Bazilevskaya et al., 2000). In the middle stratosphere an additional source of ions is due to the precipitation of relativistic electrons (RE), along field lines connecting the atmosphere with the trapped particle populations in the outer radiation belts. The Bremsstrahlung X-rays generated by the precipitating relativistic electrons penetrate down to 25-30 km altitude (Fram et al., 1997). Also, occasional solar energetic particle (SEP) events, consisting of precipitating MeV protons and alpha particles, produce ionization in the polar cap stratosphere, and on very rare occasions their energy is high enough for the ionization to extend down into the troposphere.

Because the ionosphere is charged to a potential of several hundred kilovolts by several thousand amperes of upward current flow from highly electrified clouds, the return current, which flows downward all over the globe, varies in time and geomagnetic coordinates due to the conductivity variations (e.g. Bering et al., 1998).

The downward return current density (J_z) itself affects the height distribution of ionization and conductivity as it flows through conductivity gradients and generates space charge (ρ) in accordance with Poisson's equation, $\rho = \epsilon_0 \nabla \cdot E$, where, in a horizontally stratified atmosphere $E = E_z = J_z / \sigma(z)$, so that $\rho = \epsilon_0 J_z (d/dz(1/\sigma(z)))$ with the conductivity $\sigma(z)$ varying strongly with height, and J_z being to a good approximation independent of height (Tinsley, 2000; Tinsley and Yu, 2004).

The conductivity is related to ion concentration by $\sigma = k^+ n^+ + k^- n^-$ where n^+ and n^- are the positive and negative ion concentrations, and k^+ and k^- are the positive and negative ion mobilities. The space charge is given by $\rho = n^+ - n^-$ and the total ion concentration by $n = n^+ + n^-$.

The responses of n , J_z and E_z in the global circuit to changes in GCR flux have been modeled by Roble and Hays (1979), Makino and Ogawa (1983, 1985), Tzur et al. (1983), Sapkota and Varshneya, 1990). Observations are sparse and noisy, and have been reviewed by Tinsley (1996) (see also Reiter, 1992 Fig. 6.24 and Märcz, 1997). Responses of J_z and E_z to the solar wind events originally called sector boundary crossings, and now heliospheric current sheet (HCS) crossings have been reported by Reiter (1977) and Fischer and Mühleisen (1980) and interpreted as being due to relativistic electron precipitation by Tinsley et al (1994) and Kirkland et al (1996). The interpretation is also that J_z and E_z responses at HCS crossings are only present during times of high stratospheric aerosol loading following volcanic eruptions – most recently Agung, Awu and Ferdaninda (1964-70), El Chicon (1983-86) and Pinatubo (1992-94). Data on stratospheric aerosol loading has been reviewed by Sato et al. (1993). The reason that observational data for such global circuit responses are sparse and noisy is that although these effects are important on the regional/global scale, they are weak compared to local meteorological electrical noise, especially for single point near-surface observations at low altitude on land.

Nevertheless, the study of the responses of atmospheric ionization and the global electric circuit to 'space weather' in the form of varying GCR and varying RE fluxes is important, because there appears to be a connection between such day-to-day responses and changes on the regional and global scales in cloud microphysics, affecting cloud cover and atmospheric dynamics (Tinsley, 2000; Tinsley and Yu, 2004). Because of the very different propagation times from the sun for solar wind variations as compared to solar photon variations, these day-to-day responses do not correlate with, and cannot be attributed to solar UV changes or to dynamical forcing arising from it.

Other observations of clouds associated with changes in n and J_z have been made by Marsh and Svensmark (2000); Kniveton and Todd (2001); Todd and Kniveton (2001), Kniveton and Tinsley (2004), and reviews of theories of mechanisms have been made by Carslaw et al. (2002), Harrison and Carslaw (2003), and Tinsley and Yu (2004).

Here we report on observations showing changes in atmospheric spectral transparency and in its counterpart, atmospheric extinction, associated with changes in atmospheric ionization at the time of HCS crossings and of Forbush decreases (FDs) in the GCR flux. These transparency changes are of interest because they appear to be related to the previously observed cloud and atmospheric dynamical responses to the same n , J_z and ρ changes that are discussed above.

Links between atmospheric ionization and aerosol and cloud microphysics affecting atmospheric dynamics, as observed on the day-to-day timescale, are possible

explanations for observed correlations between atmospheric ionization and climate on the decadal and centennial timescales (e.g., Donarummo et al., 2002; D'Arrigo et al., 2003) and on the millennial and hundred-million year timescales (e.g., Bond et al., 2001; Shaviv and Veizer, 2003), with or without contributions from varying solar UV irradiance (Shindell et al., 1999, 2001).

Data

Measurements of atmospheric transmission were made at a number of wavelengths from stations in the Russian Ozonsonde Network, during the years 1978-1989. Some of the 45 stations of this network were equipped with the M-3 device which measured spectral transmission P_λ of the atmosphere, where $P_\lambda = (S_\lambda/S_{0\lambda})^{1/m}$ where S_λ is the direct solar radiation with wavelength λ , and $S_{0\lambda}$ is the radiation outside the atmosphere, and m is the optical mass of the atmosphere corresponding to the solar zenith angle at the time of observation, and the formula generates the transmission as reduced to the zenith. The device has 8 glass filters with half width of about several tens of nm, and the wavelengths ranged from 326 to 627 nm. The measurements were carried out on days without visible clouds, when the Sun was more than 10° above the horizon. The error of individual measurements of P_λ is 2%. On the basis of these measurements two characteristics of the atmospheric aerosol were calculated: the optical density of the aerosol in six spectral regions and the Junge exponent, related to particle size distribution. The data have been published in year books edited by Guschin (1978-1992).

Variations in the spectral density of atmospheric aerosol at a wavelength of 369 nm have been analyzed by Roldugin and Starkov (1998, 2000) for 8 northwest stations above 55°N latitude. These stations are listed with their geographic and geomagnetic coordinates in Table 1.

For these stations they found transparency variations of a few percent that were in anticorrelation with sunspot number. An initial analysis of the time variations of extinction at 369 nm and transparency at 530 nm at the times of HCS crossings was made by Roldugin and Tinsley (2000), and here we extend this analysis and include such effects at the times of short term GCR reductions (Forbush decreases). The bandwidths of the filters at 369 nm and 530 nm were 22 nm and 60 nm.

The list of dates (key days) for which HCS crossings for 1978-1994 have been identified is taken from Kirkland et al. (1996). This period includes the interval 1983-1986 following the El Chicon eruption, when there was a high concentration of liquid $\text{H}_2\text{SO}_4/\text{H}_2\text{O}$ aerosols in the stratosphere. The work of Tinsley et al. (1994) and Kirkland et al. (1996) showed that the dynamical response of the atmosphere at HCS crossings, known as the Wilcox effect (Wilcox et al., 1973), appeared only in such periods of high stratospheric aerosol loading. They showed that at HCS crossings there are reductions of relativistic electron precipitation into the middle and high latitude upper stratosphere, and reductions in the associated X-ray Bremsstrahlung that penetrated down to about the 30 km level. Periods of high stratospheric aerosol loading begin a few months after major explosive volcanic eruptions, as the gases convert to liquid sulphate aerosol droplets and disperse throughout the stratosphere. Data on such periods are given by Sato et al. (1990, Figure 1). Consequently, the data on atmospheric transparency and extinction were divided into two groups, with the time interval 1983-86 for high aerosol loading, and the

intervals 1978-1982 plus 1987-1989 for low aerosol loading. This division of data was also used for the analysis of responses to the FDs.

The list of dates (key days) for which the FDs have been identified in neutron monitor data from Apatity is given in Table 2. This list of 81 FDs is an extension through 1989 of a similar list given by Tinsley and Deen (1991) extracted from the data of the Mt. Washington and Climax neutron monitors, but with some events excluded that were weak at Apatity, due, for example, to 'ground level' SEP events, or magnetic storm-related reductions in GCR cutoff rigidity. Events were also excluded if there is transparency data only before or only after a key day on a station; this results in a number of winter events being excluded.

The data analysis was made using the superposed epoch technique. For the HCS crossings analysis, the epochs extended from 6 days before the key (0) day to 6 days afterwards. For the FD analysis the epochs were from day -10 to day +20. Because observations were made only on cloud-free days only a small proportion (about 15%) of the total number of days in all the epochs provided data. The direct sun was observed at high zenith angles, and much of the data were obtained in summer months. Thus the transparency responses found are without regard to season, in contrast to the Wilcox effect (at HCS crossings) and the similar Roberts effect (for FDs; Tinsley, 2000) that are atmospheric dynamical responses that appear only in the northern hemisphere during the cold season (November through March).

Results

Figure 1 shows the variation of vertical atmospheric transparency at 530 nm at HCS crossings for (a) the low aerosol loading periods of 1978-82 plus 1987-89 and (b) the high loading period of 1983-86. The dotted lines are the overall means, both here and in Figure 2, and the solid lines are the separate means before and after the key day, in all four figures. For the low loading period the deviations from the mean were all less than the standard error. For the high loading period the deviation on day +2 exceeds the standard error by 4.5 standard errors. The increase in transparency on day +2 is from about 71.5% to 75.5%, or a change of about 4% in transparency. The transparency values correspond to aerosol extinction changes equivalent to a vertical optical depth change of 0.024 (i.e., 0.24 dB or 24 units of $B \cdot 10^3$). The conversion from transparency to aerosol extinction is made with allowance for Rayleigh scattering, as in Allen (1973, p. 126).

Figure 2 shows the corresponding variation of atmospheric transparency at 369 nm. Figures 1 and 2 represent essentially simultaneous measurements at two wavelengths, from which the ratio of extinctions and therefore an estimate of the particle size distributions can be made. For the high aerosol loading period (Fig 2b) day +2 has a significant deviation, by 3.7 times the standard error. Again, the low loading period (Fig 2a) shows little deviation. The increase on day +2 is equivalent to about 35 units of $B \cdot 10^3$. Comparison with the extinction change of 24 units of $B \cdot 10^3$ at 530 nm is consistent with the extinction following the $\lambda^{-1.3}$ variation characteristic of aerosol haze and dust (Allen, 1973).

The effect of FDs on transparency at 369 nm is shown for years of low stratospheric aerosol loading in Fig. 3, again as an average for all 8 stations. Here and in

figure 4 the dashed lines represent the standard error of the mean, separately before and after the key day. The mean transparency for 20 days after the key day is lower than that for the 10 days preceding it by about 1%, which is more than twice the standard error of the mean. Forbush decreases typically drop to a minimum level within one day of onset, and recover by about ten days (see Tinsley, 2000). So the shape of the variations in Fig. 3 are only roughly consistent with this pattern. An examination of individual results for each of the 8 stations revealed that the best signal/noise was at Leningrad, the station where this observational technique was developed, and best maintained. The Leningrad response is shown in Fig. 4. Averaged over 20 days the decrease following day 0 is 2.5%, and the shape of the recovery after 10 days is more consistent with the shape typical of FD recoveries. For Moscow and Arkhangelsk the decreases averaged 1%, and for Murmansk it was less than the standard error of the mean. The noise level for individual stations was such that no reliable latitude variations could be derived.

For the high aerosol period the number of observations of FDs was considerably smaller and the noise level higher. The average transmission change for all 8 stations (not shown) was less than one standard deviation of the mean.

Discussion

For the HCS crossings, the increase in transparency at 530 nm (Fig. 1) and 369 nm (Fig. 2) on day +2 for the high aerosol loading years are statistically significant. These changes occur at essentially the same time relative to the HCS crossings, and with the same duration, as the decrease in J_z at the time of HCS crossings found at Weissenau, Germany in the high stratospheric aerosol loading years of 1963-1971 (Agung and subsequent volcanic eruptions). These were all-year observations by Fischer and Mühleisen (1980) analyzed by Tinsley et al. (1994, Fig. 2). The timing and duration also agree with that of the decrease in the flux of precipitating RE (Fig. 5 of Tinsley et al., 1994) and with that of the Wilcox effect on atmospheric dynamics, as noted earlier. Because the Wilcox effect occurs only in the cold season, and the data of Figs 1 and 2 are mostly from summer months, the transparency changes cannot be a result of the Wilcox effect. The implication is that they are both forced by changes in the RE flux, through the intermediary of J_z , and that it is necessary for there to be a high aerosol loading in the stratosphere for the J_z responses to occur.

For the FDs (Figs 3 and 4) the time variations of the duration and recovery of the transparency changes, particularly for Leningrad, are similar to those of the GCR flux at FDs as discussed earlier, and imply that the changes are forced by the GCR flux. This flux causes ion production in both the troposphere and stratosphere, and so the changes in transparency could be due to changes in ion concentration n , affecting the production of ultrafine aerosols (Yu and Turco, 2001). But these are unlikely to be the source of the extinction, on account of their very small size, but could be effective if they grew to cloud condensation nuclei size, when they could act as nuclei for haze particles, or ice crystals, forming subvisible clouds.

Changes in the GCR flux cause a latitudinal redistribution in the current density J_z in the global electric circuit (Tinsley, 1996, 2000). Thus the changes in transparency associated with FDs could also be due to changes in J_z , producing space charge ρ at conductivity gradients where stratification exists in aerosol or water vapor content, or in

temperature or pre-existing sub-visible liquid or ice clouds. With changes in ρ there could be changes in either the electroscavenging process or in the ion-mediated nucleation process (Tinsley and Yu, 2004) that affect the sub-visible cloud or haze properties.

Since the transparency change associated with FDs was present in the low aerosol load years, and was absent or compensated for in the high load years, the result for low load years appears to be due to a process independent of stratospheric volcanic aerosols. This points to the tropopause region or the troposphere as the location of the extinction.

The amount of change of transmission at HCS crossings for high aerosol load years can be compared with the optical depth measured by satellites for those years at latitudes above 55°N. Using the data from Sato et al. (1993) for a wavelength of 550 nm, an estimate for the stratospheric optical depth down to 2 km above the tropopause averaged for the high load years is about .035 and for the low load years about .005, so that the difference of .03 can be compared to the change of .024 on day +2 inferred from Fig 1. If all the effects were in the stratosphere it would be necessary that essentially all the stratospheric aerosol disappeared on day +2, which seems implausible, especially as transparency changes were also found in years without high loads of stratospheric aerosols, as in Figs 3 and 4. So again, the more plausible scenario is for changes in the troposphere or tropopause region where the extinction could be due to haze and subvisible water and ice clouds. The role of the stratospheric H₂SO₄/H₂O aerosols would then be to ensure a high enough stratospheric column resistance in the absence of RE and X-ray fluxes, so that the changes in stratospheric conductivity caused by the presence of these fluxes were sufficiently large to modulate J_z so that it could affect electroscavenging or ion-mediated nucleation processes in the troposphere or tropopause region. The difference in responses for FDs as compared with HCS crossings could perhaps be due to changes in ion production and n accompanying the J_z changes for FDs but not for HCSs, together with the presence of some H₂SO₄ aerosols and vapor in the troposphere and tropopause region in the high aerosol load years.

The change in transparency for both the FDs and HCS crossings is a few percent, and this is roughly the amount of change found by Roldugin and Starkov (1998, 2000) for an 11-year cycle that is anticorrelated with sunspot number, and positively correlated with GCR flux. This is the same sense of correlation as in Figs. 3 and 4. In the light of the present results it seems likely that the 11-year transparency cycle is forced by the same mechanism as these short term variations. Although it was earlier concluded that the correlation was better with sunspot number than with GCR flux, that distinction appears not to be statistically significant.

These decadal transparency variations, if present over all high latitude regions, are large enough to produce observable climate changes. It was noted by Dickinson (1975) that a change in upper level cloud opacity by 20% would produce heating rates in the column below of order 0.1°C/day, which as a differential across a zone 15° in latitude would lead to changes in zonal winds at tropopause altitudes of the order of 2 m s⁻¹.

The identification of the mechanism(s) involved would be greatly aided by independent data that provides height resolution on the extinction. Data from middle and high geomagnetic latitudes would be needed. Day-to-day variations in lidar backscatter measurements at short wavelengths at mid-high geomagnetic latitudes would be very informative. Additional data could come from analyses of day-by-day variations in

satellite measurements of aerosol extinction, that should allow separate evaluation of transmission variations in the tropopause region as compared to those from higher altitudes. It would be helpful to obtain data on atmospheric transparency from observations at other high latitude ozone or astronomical observatories outside the Russian network, and for the Agung and Pinatubo, as well as the El Chicon epochs and for other times. This would improve the signal/noise, show latitude variations, and show how the extinction varied for intermediate stratospheric aerosol loadings for both the HCS and the FD responses.

The development of extended modeling of electroscavenging and ion-mediated nucleation covering the range of temperatures and pressures for the troposphere and stratosphere would be useful, for a wide range of H₂SO₄ mixing ratios and concentrations of background aerosol particles.

Conclusions

Changes in atmospheric transparency have been observed that accompany inferred changes in ionosphere-earth current density J_z . The presence of the effect with Forbush decreases in years without stratospheric volcanic aerosols implies changes in the tropopause or troposphere region. The particle size distribution inferred from the wavelength dependence of the spectral extinction, and the amount of the extinction, imply changes in subvisible haze, water or ice clouds in that region. The nature of the transparency changes appears to depend on the amounts of stratospheric H₂SO₄ aerosol particles that are present in the atmosphere, and whether or not changes in J_z are accompanied by ion production changes due to cosmic ray flux changes. Mechanisms that have been theorised to involve the effect of electric charge on the formation of aerosols, and/or of the effects of electroscavenging of charged aerosols on phase conversions between water vapor, liquid water, and ice may have some relevance to these transparency changes. Improved observational data and improved modeling of the microphysical effects of charged aerosols are clearly needed if our understanding of this phenomenon is to be improved.

Acknowledgements

This work has been supported by NSF ATM grants 9903424 and 0242827

References

- Allen, C. W., 1973. *Astrophysical Quantities*, 3rd ed., Althone Press, London.
- Bazilevskaya, G. A., Krainev, M. B., Makhmutov, V. S., 2000. Effects of cosmic rays on the Earth's environment, *J. Atmos. Solar Terr. Phys.*, 62, 1577-1586.
- Bering, E. A. III, Few, A. A., Benbrook, J. R., 1998. The global electric circuit, *Physics Today*, 51, 24-30.
- Bond, G., Kromer, B., Beer, J., Muscheler, R., Evans, M. N., Showers, W., Hoffman, S., Lotti-Bond, R., Hajdas, I., Bonani, G., 2001. Persistent solar influence on North Atlantic climate during the Holocene, *Science*, 294, 2130-2136.
- Carslaw, K. S., Harrison, R. G., Kirby, J., 2002. Cosmic rays, clouds, and climate, *Science*, 298, 1732-1737.

- D'Arrigo, R. D., Cook, E. R., Mann, M. E., Jacoby, G. E., 2003. Tree ring reconstructions of temperature and sea-level pressure variability associated with the warm-season Arctic Oscillation since AD 1650, *Geophys. Res. Lett.*, 30(11) 1549, doi:10.1029/2003GL017250.
- Dickinson, R. E., 1975. Solar variability and the lower atmosphere, *Bull. Am. Meteorol. Soc.*, 56, 1240-1248.
- Donarummo, J. Jr., Ram, M., Stolz, M. R., 2002. Sun/dust correlations and volcanic interference, *Geophys. Res. Lett.*, 29(9), 75, doi10.1029/2002GL014858.
- Fram, R. A., Winningham, J. D., Sharber, J. R., Link, R., Crowley, G., Gaines, E. E., Chenette, D. L., Anderson, B. J., Potemera, T. A., 1997. The diffuse aurora, a significant source of ionization in the middle atmosphere, *J. Geophys. Res.*, 102, 28,203 – 28,214.
- Fischer, H. J., Mühleisen, R., 1980. The ionospheric potential and the solar magnetic sector boundary crossings, Rept. Astronom. Inst. Univ. Tübingen, Ravensberg, Germany.
- Guschin, G. P., (ed.), 1978-1992. Common content of atmospheric ozone and spectral transparency of atmosphere, Annual data reports (in Russian). Hidrometeorizdat, Leningrad.
- Harrison, R. G., Carslaw, K. S., 2003. Ion-aerosol-cloud processes in the lower atmosphere, *Rev. Geophys.*, 41(3), 1012, doi10.1029/2002RG000114.
- Kniveton, D. R., Tinsley, B. A., 2004. Daily changes in global cloud cover and Earth transits of the heliospheric current sheet, in press, *J. Geophys. Res.-Atmospheres*.
- Kniveton, D. R., Todd, M. C., 2001. On the relationship of cosmic ray flux and precipitation, *Geophys. Res. Lett.*, 28, 1527-1530.
- Kirkland, M., Tinsley, B. A., Hoeksema, J. T., 1996. Are stratospheric aerosols the missing link between tropospheric vorticity and Earth transits of the heliospheric current sheet?, *J. Geophys. Res.*, 101, 29,689-29,699
- Makino, M., Ogawa, T., 1983. Interpretation of the solar flare modification of atmospheric electric field and air-earth current, in B. M. McCormac (ed), *Weather and Climate Responses to Solar Variations*, Colo. Assoc. Univ. Press, Boulder, pp. 419-426.
- Makino, M., Ogawa, T., 1985. Quantitative estimation of global circuit, *J. Geophys. Res.*, 90(D4), 5961-5966.
- März, F., 1997. Short term changes in atmospheric electricity associated with Forbush decreases, *J. Atmos. Solar Terr. Phys.*, 59, 975-982.
- Marsh, N., Svensmark, H., 2000. Low cloud properties influenced by cosmic rays, *Phys. Rev. Lett.*, 85, 5004-5007.
- Reiter, R., 1977. The electric potential of the ionosphere as controlled by the solar magnetic sector structure; result of a study over the period of a solar cycle, *J. Atmos. Terr. Phys.*, 39, 95-99.
- Reiter, R., 1992. *Phenomena in Atmospheric and Environmental Electricity*, Elsevier, Amsterdam.
- Roble, R. G., Hays, P. B., 1979. A quasi-static model of global atmospheric electricity, II. Electrical coupling between the upper and the lower atmosphere, *J. Geophys. Res.*, 84, 7247-7256.
- Roldugin, V. C., Starkov, G. V., 1998. Dependence of atmospheric transparency variations on solar activity, *Studia Geophys. et Geod.*, 42(2), 137-146.

- Roldugin, V. C., Starkov, G. V., 2000. Atmospheric transparency changes during 11 year solar cycle, (in Russian), *Doklady Akademii Nauk*, 370(5), 675-677. English translation: *Doklady Earth Sciences*, 2000, 371(2), 304-306.
- Roldugin, V. C., Tinsley, B. A., 2000. Changes of atmospheric aerosol density after Earth-transits of the heliospheric current sheet, *Proceedings of the Apatitian XXIII Seminar 2000, Auroral Phenomena*, Polar Geophysical Institute, Apatity, Russia.
- Sapkota, B. K., Varshneya, N. C., 1990. On the global atmospheric electrical circuit, *J. Atmos. Terr. Phys.*, 52, 1-20.
- Sato, M., Hansen, J. E., McCormick, M. P., Pollack, J. B., 1993. Stratospheric aerosol optical depths, 1850-1990, *J. Geophys. Res.*, 98(D12), 22,987-22,994.
- Shindel, D., Rind, D., Balachandran, N., Lean, J., Lonergan, P., 1999. Solar cycle variability, ozone and climate, *Science*, 284(5412), 305.
- Shindel, D. T., Schmidt, G. A., Mann, M. E., Rind, D., Waple, A., 2001. Solar forcing of regional climate change during the Maunder Minimum, *Science*, 294, 2149-2152.
- Shaviv, N. J., Veizer, J., 2003. Celestial driver of Phanerozoic climate?, 2003. *GSA Today*, July 2003, 4-10.
- Todd, M. C., Kniveton, D. R., 2001. Changes in cloud cover associated with Forbush decreases of galactic cosmic rays, *J. Geophys Res.*, 106, 32,031-32,041.
- Tzur, I., Roble, R. G., Zhuang, H. C., Reid, G. C., 1983. The response of the Earth's global electric circuit to a solar proton event, in B. M. McCormac (ed), *Weather and Climate Responses to Solar Variations*, Colo. Assoc. Univ. Press, Boulder, pp. 427-435.
- Tinsley, B. A., 1996. Correlations of atmospheric dynamics with solar wind-induced changes of air-earth current density into cloud tops, *J. Geophys. Res.*, 101, 29,701-29,714.
- Tinsley, B. A., 2000. Influence of the solar wind on the global electric circuit, and inferred effects on cloud microphysics, temperature, and dynamics of the troposphere, *Space Science Reviews*, 94, 231-258.
- Tinsley, B. A., Deen, G. W., 1991. Apparent tropospheric response to MeV-GeV particle flux variations: A connection via electrofreezing of supercooled water in high level clouds? *J. Geophys. Res.*, 96, 22283-22296.
- Tinsley, B. A., Yu, F., 2004. Atmospheric ionization and clouds as links between solar activity and climate, pp. 321-340 in *Solar Variability and its Effects on Climate*, AGU Monograph 141, ed. J. Pap et al., AGU press, Washington, DC.
- Tinsley, B. A., Hoeksema, J. T., Baker, D. N., 1994. Stratospheric volcanic aerosols and changes in air-earth current density at solar wind magnetic sector boundaries as conditions for the Wilcox tropospheric vorticity effect, *J. Geophys. Res.*, 99, 16,805 - 16,813.
- Wilcox, J. M., Scherrer, P. H., Svalgaard, L., Roberts, W. O., Olson, R. H., 1973. Solar magnetic sector structure: Relation to circulation in the Earth's atmosphere, *Science*, 180, 185-186.
- Yu, F., Turco, R. P., 2000. Ultrafine aerosol formation via ion-mediated nucleation, *Geophys. Res. Lett.*, 27, 883-886.

Table 1. Geographic and corrected geomagnetic coordinates of the stations

Station	Geog. Lat.	Geog. Long.	Geomag. Lat.	Geomag. Long.
Arkhangelsk	64° 35'	40° 30'	60.6°	118.0°
Leningrad	59° 58'	30° 18'	55.7°	108.1°
Markovo	64° 41'	170° 25'	59.3°	232.1°
Moscow	55° 45'	37° 34'	50.8°	111.9°
Murmansk	68° 58'	33° 03'	64.5°	115.2°
Nagayevo	59°35'	150° 47'	53.3°	218.8°
Pechora	65° 07'	57° 06'	61.6°	132.6°
Sverdlovsk	56° 48'	60° 38'	52.0°	132.6°

Table 2. List of key days defining Forbush decreases

1972 03 06	1974 05 14	1978 06 26	1980 03 05	1981 05 15	1984 04 26
1972 03 27	1974 05 31	1978 07 13	1980 04 03	1981 05 18	1985 04 26
1972 05 15	1974 07 06	1978 09 24	1980 06 08	1981 07 23	1985 07 12
1972 05 30	1974 09 13	1978 09 29	1980 06 23	1981 08 10	1986 03 09
1972 06 17	1975 03 26	1979 02 18	1980 07 25	1982 03 01	1988 08 26
1972 08 04	1976 05 21	1979 03 28	1980 09 02	1982 04 13	1989 03 13
1972 10 18	1977 09 22	1979 04 05	1980 09 05	1982 04 25	1989 04 12
1972 10 31	1978 02 15	1979 04 25	1980 11 10	1981 06 09	1989 08 10
1973 01 19	1978 03 08	1979 06 06	1981 02 24	1982 07 13	1989 08 14
1973 04 13	1978 04 03	1979 07 06	1981 03 01	1982 08 06	1989 09 05
1973 05 07	1978 04 10	1979 08 01	1981 03 26	1982 09 06	1989 09 19
1973 05 13	1978 04 18	1979 08 20	1981 03 31	1982 09 21	
1973 07 13	1978 05 01	1979 09 17	1981 04 02	1983 03 10	
1974 03 22	1978 06 02	1979 10 06	1981 05 11	1984 02 26	

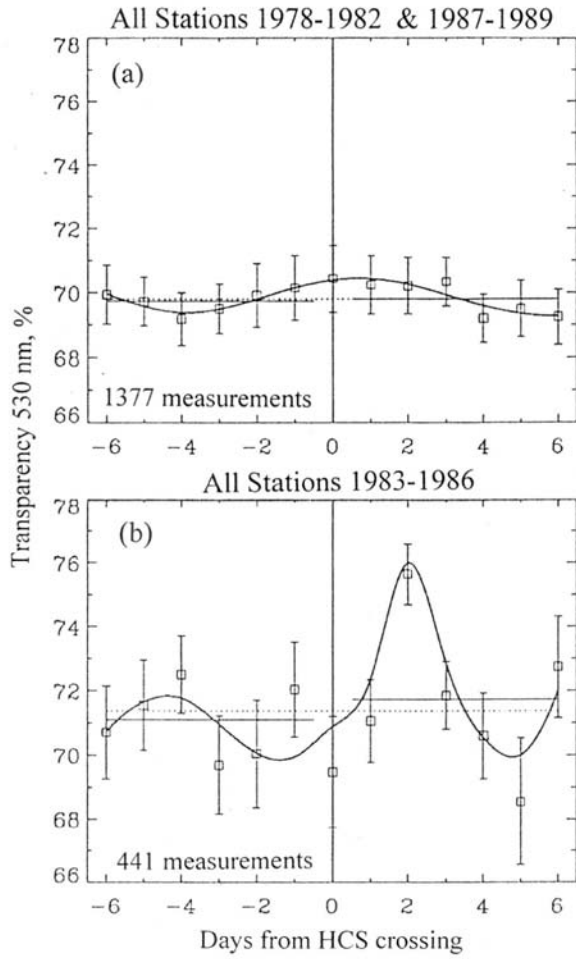


Figure 1. Superposed epoch analysis of atmospheric transparency at 530 nm, with the zero day being that of HCS crossings, for all 8 stations listed in the text, for (a) years of low stratospheric aerosol loading, and (b) years of high stratospheric aerosol loading.

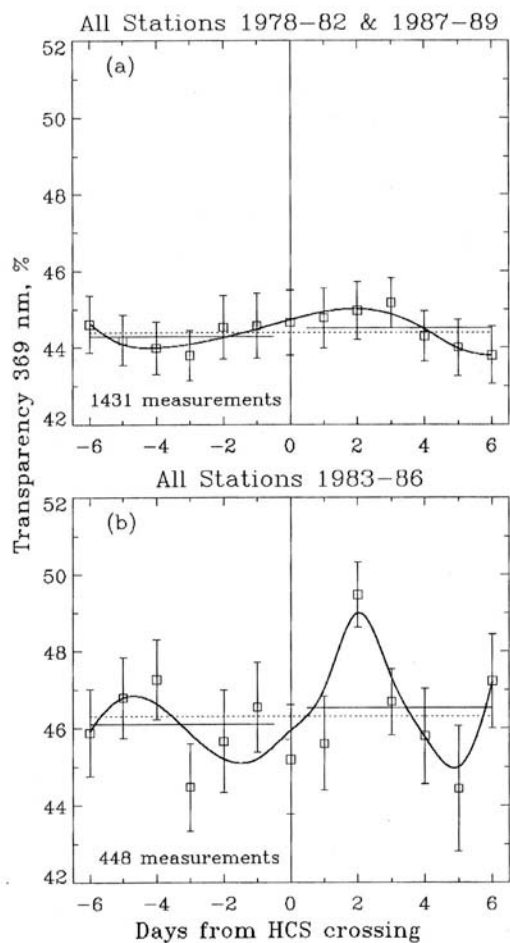


Figure 2. As for Figure 1 for 369 nm.

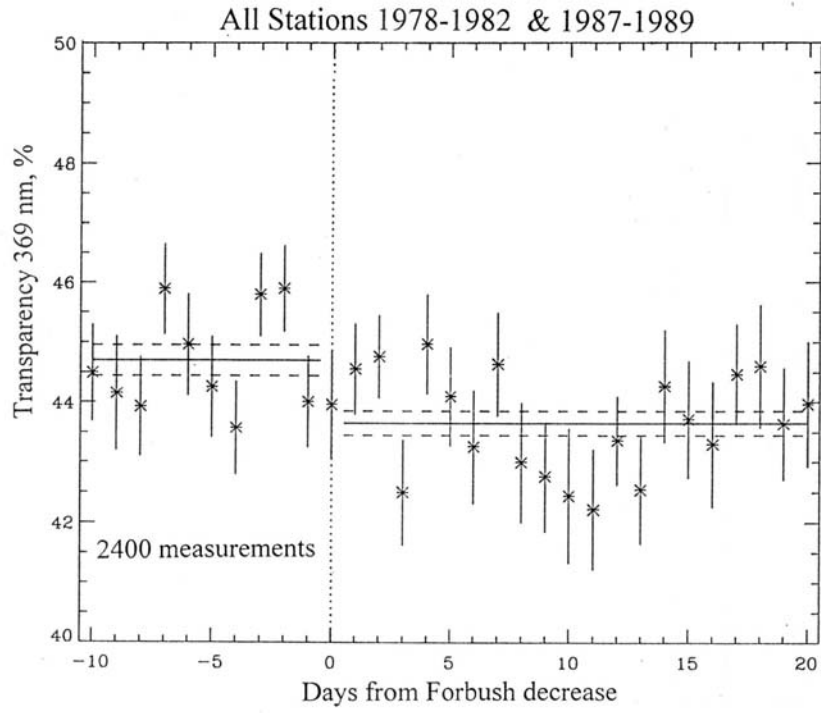


Figure 3. Superposed epoch analysis of atmospheric transparency at 369 nm, with the zero day being that of Forbush decreases of the galactic cosmic ray flux, averaged for all stations, for years of low stratospheric aerosol flux.

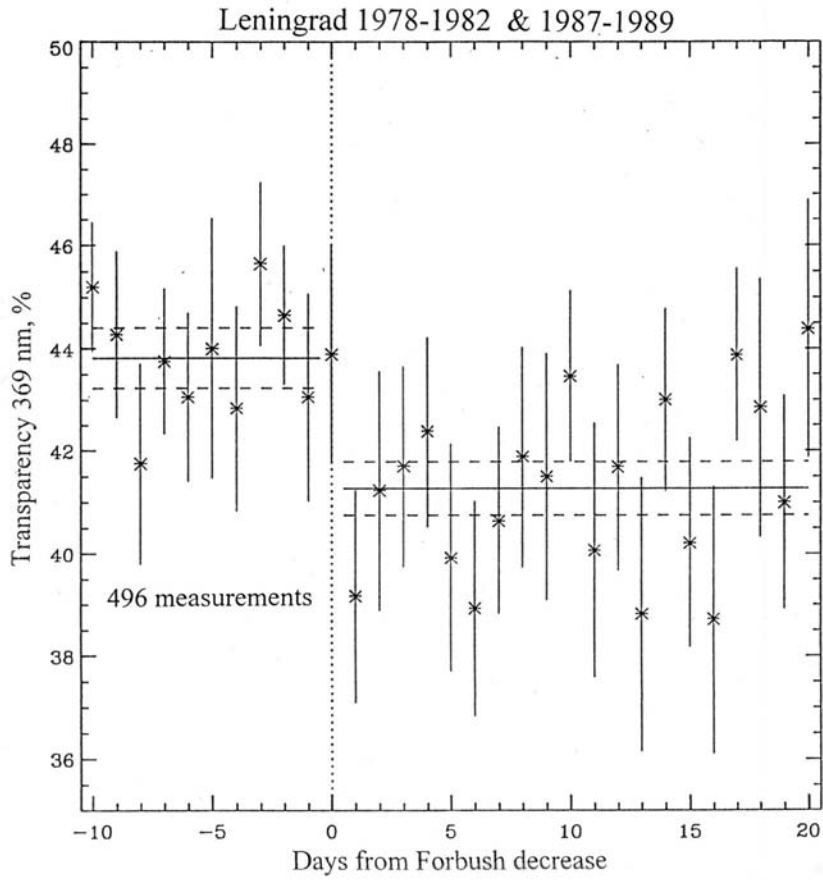


Figure 4. Superposed epoch analysis of atmospheric transparency at 369 nm, with the zero day being that of Forbush decreases of the galactic cosmic ray flux, as measured from Leningrad, for years of low stratospheric aerosol loading.